Determinant Selection of Major Histocompatibility Complex Class I-restricted Antigenic Peptides Is Explained By Class I-peptide Affinity and Is Strongly Influenced by Nondominant Anchor Residues

By Weisan Chen,* Sergei Khilko,‡ John Fecondo,§ David H. Margulies,‡ and James McCluskey*

From the *Centre for Transfusion Medicine & Immunology, Flinders Medical Centre, Bedford Park, South Australia, 5042, Australia; the ‡Laboratory of Immunology, National Institutes of Allergy and Infectious Diseases, National Institutes of Health, Bethesda, Maryland 20892; and the §Department of Applied Chemistry, Swinburne University of Technology, Hawthorn, Victoria, 3122, Australia

Summary

The contribution of major histocompatibility complex (MHC) class I–peptide affinity to immunodominance of particular peptide antigens (Ags) in the class I–restricted cytotoxic T lymphocyte (CTL) response is not clearly established. Therefore, we have compared the H-2K^b-restricted binding and presentation of the immunodominant ovalbumin (OVA)$_{257-264}$ (SIINFEKL) determinant to that of a subdominant OVA determinant OVA$_{55-62}$ (KVVRFDKL). Immunodominance of OVA$_{257-264}$ was not attributable to the specific T cell repertoire but correlated instead with more efficient Ag presentation. This enhanced Ag presentation could be accounted for by the higher affinity of K^b/OVA$_{257-264}$ compared with K^b/OVA$_{55-62}$ despite the presence of a conserved K^b-binding motif in both peptides. Kinetic binding studies using purified soluble H-2K^b molecules (K^b$_s$) and biosensor techniques indicated that the K$_{on}$ for association of OVA$_{257-264-C6}$ and K^b$_s$ at 25°C was ~10-fold faster (5.9 × 10^3 M^{-1} s^{-1} versus 6.5 × 10^2 M^{-1} s^{-1}), and the K$_{off}$ approximately twofold slower (9.1 × 10^{-6} s^{-1} versus 1.6 × 10^{-5} s^{-1}), than the rate constants for interaction of OVA$_{55-62-C6}$ and K^b$_s$. The association of these peptides with K^b was significantly influenced by multiple residues at presumed nonanchor sites within the peptide sequence. The contribution of each peptide residue to K^b-binding was dependent upon the sequence context and the summed contributions were not additive. Thus the affinity of MHC class I–peptide binding is a critical factor controlling presentation of peptide Ag and immunodominance in the class I–restricted CTL response.

M HC class I molecules act as receptors for endogenous Ags by assembling with peptide fragments created in the cytoplasm and then delivered to a pre-Golgi compartment. Peptides associated with class I molecules are generally 8–10 amino acids in length (1–3) and are imported into the vacuolar system via multidrug-resistant pumplike molecules (transporter associated with Ag processing [TAP] molecules) encoded within the MHC (4–7). The factors likely to control which peptide Ags are presented to class I–restricted T cells include the processing machinery which creates cytosolic peptides (8), selectivity in the transport of peptides by TAP molecules (9, 10), and the affinity of peptide interaction with class I molecules. In class II–restricted immunity, responsiveness to particular peptides correlates strongly with the capacity of these peptides to bind the relevant class II molecule (11–13). Although early class I studies were limited

by the nature of the binding assays (14–16), a number of recent reports have refined the approach to measuring MHC class I–peptide binding and have demonstrated specificity of MHC class I–peptide association (17–20) and a preference for peptides of optimal length (21–26). Kinetic studies suggest significant differences occur in the association and dissociation rates of different peptide–MHC class I complexes (21, 25, 27), but it is unclear how these differences might affect peptide presentation. Other studies have attempted to quantitate the contribution of the individual peptide residues in peptide–MHC class I binding (23, 24, 28). In an analysis of the affinities of various peptides for K^b, the free energy contribution of the dominant anchor side chains was found to be unexpectedly large suggesting a crucial role for these residues in specific high affinity binding (24). In contrast, studies of peptide binding to HLA-A2.1 molecules found that anchor

residues were necessary but not sufficient for high affinity binding and that secondary anchor sites played a prominent role in controlling the association of peptides with class I molecules (26). It is not clear, however, whether these influences on peptide–MHC class I binding observed in vitro actually influence determinant selection and CTL response in vivo. This is largely because MHC class I–peptide binding studies have focussed on defined antigenic peptides or their analogues and have not directly correlated the peptide binding parameters with the patterns of determinant selection and immunodominance in the class I–restricted CTL response in vivo.

To examine this relationship between the CD8+ CTL response in vivo and class I–peptide binding we have compared the H-2K^b–restricted binding and presentation of the immunodominant determinant from chicken OVA$_{257-264}$ to that of a newly identified subdominant determinant, OVA$_{55-62}$ derived from the same protein and restricted by the same MHC molecule (K^b). Our findings indicate that immunodominance can be accounted for by higher affinity peptide binding to class I molecules, which is associated with more efficient Ag presentation by APCs. Moreover, the differential class I–peptide binding affinities of OVA peptides are the result of kinetic variation in both the association and dissociation rates of MHC class I–peptide complexes which are controlled by differences in nondominant anchor residue sites within the peptide Ag.

Materials and Methods

Cell Culture. The thymoma cell line EL-4 (H-2^b) (TIB39; American Type Culture Collection, Rockville, MD; 29), the TAP2 mutant cell line RMA-S (H-2^b) (29), and the OVA-transfected EL-4 cell line EG7 (30) were described elsewhere. The OVA1-1 cell was created by transfecting the H-2K^b–expressing L cell I-3 (H-2^k, H-2K^b) with pAC-neo-OVA gene (30) using the calcium phosphate method. G418 (Geneticin; GIBCO BRL, Gaithersburg, MD) was added to the culture to a final 0.3–0.5 mg/ml (active concentration) 24 h after transfection. Cells were then cloned by limiting dilution. HGPRT-negative BW5147-Lyt2.4 cells used for hybridoma fusions express a neomycin resistant marker gene which maintains the selection of Lyt2.4 (CD8) (31).

Cultured cell lines were grown in DMEM containing 10% FCS (DME-10), 5 × 10^{-5} M 2-ME, antibiotics, and 2 μM glutamine. Spleen cells were freshly prepared and irradiated with 3,000 rad before use as APCs.

Priming CTL In Vitro. CTL priming, restimulation, and T-T hybridoma fusion were performed in RPMI-1640 medium containing 10% FCS (RP-10) with the same supplements as above. Primary CTL cultures were established by sensitizing 5 × 10^7 syngeneic spleen cells from female C57BL/6 (H-2^b) mice with 5 × 10^7 irradiated, and OVA-electroporated (2 mg/ml) spleen cells in an upright T-25 flask (32). After 5 d, the live responder cells were recovered from a Ficoll-Hypaque gradient and restimulated in 24-well plates at a density of 5 × 10^5/well with 5–10 U/ml rIL-2. Each well received 2.5 × 10^6 irradiated spleen cells as feeders and the same number of electroporated stimulators. The responder T cells were restimulated after 5 d, and their CTL activity was then tested in a routine ^{51}Cr-release assay. For the primed CTL

precursor (CTLp)[1] assays spleen cells (5 × 10^7) from C57BL/6 mice were electroporated in the presence of 5 mg/ml native OVA. Cells were then washed once before intravenous injection into syngeneic mice. 10 d later, in vivo primed spleen cells were titrated at the following cell densities: 8, 4, 2, 1, 0.5, and 0.25 × 10^5 cells in each microtiter well with 2.5 × 10^5 irradiated spleen cells as feeders and a similar number of OVA-electroporated (5 mg/ml) spleen cells as stimulators. The cultures were incubated for 8 d in RP-10 medium. Recombinant IL-2 was added to the cultures in fresh medium at a final concentration of 5–10 U/ml from day 4. The IL-2-containing medium was replaced by normal medium 12–16 h before the standard ^{51}Cr-release cytotoxicity assay to avoid lymphokine-activated killing (LAK). RMA-S cells grown at 25°C overnight were used as targets (33). 24 wells of each cell density were assayed for cytotoxicity on RMA-S, OVA$_{257-264}$–pulsed RMA-S and OVA$_{55-62}$–pulsed RMA-S cells. Positive wells were scored if cytotoxicity exceeded the spontaneous release plus three standard deviations. The fraction of negative wells was plotted against starting splenic cell density according to Poisson distribution to derive the CTLp values at 37% negative wells (34). The CTLp frequency values derived from this assay reflect CTL per splenocyte, noting that about one third of spleen cells are T cells (35).

T-T Hybridoma Fusion and Ag Presentation Assays. Cell fusion was carried out in 42% polyethylene glycol (PEG) (mol wt 1,500, BDH Chemicals, Kilsyth, Australia) and 15% DMSO. Responder T cells were separated on Ficoll-Hypaque to remove dead cells and cell debris, then washed and fused with BW5147-Lyt2.4 fusion partner cells at a ratio of 5 to 1. Approximately 24 h after fusion, 50 μl of 3× HAT medium was added to each well, and after another 24 h, 50 μl of G418-containing HAT medium was added. The final concentration of HAT was hypoxanthine 100 μM, aminopterin 0.4 μM, and thymidine 16 μM; G418 was 0.3 mg/ml. Expanded clones were cocultured with OVA$_{55-62}$–pulsed APCs and the supernatants were assayed for IL-2 using the cell line CTLL (36). The positive clones were also tested by assaying their dose responsiveness and surface expression of TCR and CD8. Clone 1G8 was the most sensitive clone obtained from the fusion (data not shown). For Ag presentation assays involving OVA (grade VI; Sigma Chemical Co., St. Louis, MO), APCs were loaded with Ag by electroporation, commercial liposomes, or osmotic loading as described (30, 32).

Peptide Synthesis. For initial screening of CTL activity, a set of OVA 15-mer peptides was synthesized by the Multipin Synthesis System (Chiron Mimotopes, Clayton, Australia; 37) and dissolved in DMSO at about 1 mM. All other octamer peptides were assembled on a peptide synthesizer (model 431A; Applied Biosystems, Foster City, CA), using highly optimized *tert*-butyloxycarbonyl) (*t*-Boc) solid phase synthesis chemistry protocols. The peptides were deprotected and cleaved from PAM resin using standard high-fluoride (HF) methods, followed by extraction into 10–30% acetic acid. OVA$_{257-264}$, OVA$_{55-62}$, OVA$_{54-62}$, OVA$_{257-264-C6}$, OVA$_{55-62-C6}$, OVA$_{257-264-C4}$, and OVA$_{55-62-C4}$ were purified to >95% purity by semipreparative reverse phase HPLC using an Aquapore C8 column on a high performance liquid chromatographer (model 160A; Applied Biosystems). Final characterization and assessment of purity was achieved by reverse phase HPLC or by capillary electrophoresis (model 270A; Applied Biosystems). All peptides and

---

[1] *Abbreviations used in this paper:* BFA, brefeldin A; CTLp, CTL precursor; ER, endoplasmic reticulum; HBST, Hepes Buffered Saline Tween; SPR, surface plasmon resonance.

analogues were dissolved in PBS at 400 μM as stock solutions and kept at $-20°$C.

Peptide Binding to K^b on RMA-S Cells. Relative peptide binding to H-2K^b was assessed by measuring the folding and stabilization of K^b on the surface of RMA-S cells after culture in medium containing the appropriate peptides (17, 38, 39). RMA-S cells (3 × 10^5) were incubated at 25°C for 12–14 h in 400 μl DME-10 and graded concentrations of peptides were added for the last 60 min before transfer of the cells to 37°C for 2 h to allow the "empty" molecules to disappear from the cell surface. The cells were then harvested and stained on ice using a conformational K^b-specific antibody, Y3 (17), or an α1-domain–specific antibody, 20.8.4 (40) and analyzed by FACScan$^®$ (Becton Dickinson & Co., Mountain View, CA). Peptide binding to K^b resulted in a proportional increase in mean channel fluorescence of mAb staining. To estimate the relative dissociation rates of peptides bound to RMA-S cells, these cells were set up in 12-well plates at a density of 1.2 × 10^6/ml in the presence or absence of 10 μM peptides for 12 h at 25°C. Brefeldin A (BFA) (10 μg/ml) was added to the cultures for the last 2.5 h to prevent the appearance of newly synthesized class I molecules (41). The cells were then washed with prewarmed medium, before being aliquoted into 0.3-ml volumes of DME-10 containing 10 μg/ml BFA and subsequently transferred to a 37°C incubator. This time point was taken as time zero. At different time points afterwards, samples were collected and directly stained for K^b-peptide complexes on the cell surface with mAb 20.8.4. RMA-S cells cultured under the same conditions but with BFA continuously present in the medium were also studied. BFA inhibits the egress of newly synthesized class I molecules from the endoplasmic reticulum (ER) to the cell membrane (41).

Flow Cytometry. Cells were harvested and washed in PBS. These cells (3 × 10^5) were then incubated with either 100 μl of PBS containing 5% FCS or mAb culture supernatants for 30 min on ice. Washed cells were then incubated with fluoresceinated sheep anti–mouse Ig (Silenus Labs. Pty., Ltd., Hawthorn, Victoria, Australia), washed in PBS, and resuspended in FACS$^®$ fixative containing 1% paraformaldehyde and 0.02% azide (0.15–0.2 ml/tube). For each histogram, 10,000 viable cells were counted on a FACScan$^®$.

Peptide Competition Assays. Both OVA$_{257-264}$ and OVA$_{55-62}$ peptides were freshly diluted from stock solutions to ~3 × 10^{-11} M in DMEM free of FCS as stimulator peptides. These solutions were then used as solvent to dilute the competitor peptides to various concentrations ranging from 10^{-5} to 10^{-15} M. I-3 cells were set up in 96-well plates at 2 × 10^4/well in DME-10 overnight. The overnight medium was completely removed and 50 μl of stimulator/competitor peptide mixture was added to each well. Cells were pulsed for 30 min at 37°C in a CO$_2$ incubator. Then the peptide mixture was removed and the cells were washed three times with serum-free DMEM. T hybridoma cells (10^5) were added into each well and supernatants from a 24-h coculture were then assayed for IL-2 content.

MHC Class I Molecules. The engineered, soluble murine MHC class I molecule H-2K^b, was produced in transfected L cells and purified by immunoaffinity chromatography as described previously (42). To increase the peptide binding capacity, H-2K^b, was emptied of endogenous peptides by exposure to pH 12.5, 0.2 M potassium phosphate buffer for 10 min on ice and was neutralized by centrifugation through a column (Bio-Spin 6; Bio-Rad Laboratories, Richmond, CA) equilibrated with 20 mM Hepes, pH 7.3, 0.15 M NaCl, 3.4 mM EDTA, and 0.005% Tween-20 (Hepes Buffered Saline Tween [HBST]).

Surface Plasmon Resonance. For real time binding experiments,

a biosensor system (BIAcore^{TM}; Pharmacia Biosensor, Piscataway, NJ) was used (43). Binding of soluble macromolecules to a ligand immobilized on a dextran-gold surface results in changes in the surface plasmon resonance (SPR) signal recorded in real time. All biosensor binding experiments were carried out in HBST buffer. Details of the use of the biosensor system to detect peptide–MHC interaction have been described elsewhere (20). The analogues of the OVA-derived peptides substituted with cysteine at position 6 (OVA$_{257-264-C6}$, SIINFCKL and OVA$_{55-62-C6}$, KVVRFCKL) were immobilized to the carboxymethyl dextran surface of the biosensor using a slightly modified approach described previously as Method D (20).

SPR Binding Experiments. Soluble, immunoaffinity purified H-2K^b, molecules were diluted to concentrations between 0.625 μM (39 μg/ml) and 5 μM (312.5 μg/ml) in HBST and exposed to the peptide-modified surfaces. After each binding cycle, the surface was regenerated by injection of 50 mM phosphoric acid for 30 s. For the association rate analysis, 40 μl of the protein solution was injected at a flow rate of 5 μl/min. For the dissociation rate measurement, 40 μl of the H-2K^b, solution was injected at 1 μl/min to load the peptide surface, and the dissociation phase was carried out by injection of HBST at 100 μl/min for a period of 80 min. The SPR signal obtained in each binding cycle was recorded as a real time pattern with a sampling interval of 0.2–0.5 s plotted in resonance units (RU) versus time. This plot is known as a "sensorgram."

Estimation of Kinetic Rate Constants. The sensorgrams were transferred as text files to a Macintosh computer (model IIfx; Apple Computer, Inc., Cupertino, CA) and curve fitting was performed using IGOR Graphing and Data Analysis software (WaveMetrics, Lake Oswego, OR). The baseline of each sensorgram was corrected by subtraction of the SPR signal before the injection of the protein. For determination of the association rate constant, the association phase of the sensorgram was fitted to a double exponential formula: $B_t = B_{tot} - B_m\text{prot}[\exp(-k1_{obs}t)] - B_m\text{buf}[\exp(-k2_{obs}t)]$, where $B_m\text{prot}$ corresponds to maximal protein binding available, and $k1_{obs}$ to a product of the kinetic association rate constant, k_{as} and the concentration of empty molecules of H-2K^b, c. Formally, $k1_{obs} = K_{as} c + k_{dis}$, but in this case, since k_{dis} is $\ll k_{as} c$, it does not significantly influence the fit (see Results). The second exponential term was introduced to compensate for the rapid rise of the resonance signal during the first seconds of the injection as a result of the buffer change. For each of the peptide surfaces, $k1_{obs}$ values were obtained at three different H-2K^b, concentrations and plotted as a function of the concentration. The slope of this graph was taken as the kinetic association rate constant, k_{as}. The dissociation part of the sensorgrams was fitted to the double exponential equation: $B_t = B_o^{fast} \exp(-k_{dis}^{fast} t) + B_o^{slow} \exp(-k_{dis}^{slow} t)$, where B_t corresponds to binding (in RU) at time t. Assuming two classes of dissociating complexes, B_o for each class corresponds to binding at time zero, and k_{dis} to the kinetic dissociation rate constant (s^{-1}), whereas "fast" and "slow" indicate the two kinetic classes.

Results

OVA-specific CTLs Recognize Multiple OVA Determinants in H-2^b Mice. In H-2^b mice challenged with OVA by cross-priming (44), osmotic loading of cells with OVA (45) or immunization with the EL-4 OVA-transfectant EG7, the OVA-specific CTL response is dominated by T cells specific for OVA$_{257-264}$ (30, 44, and data not shown). However, when

mice were immunized by injection of spleen cells electroporated with a high concentration (2 mg/ml, 45 μM) of freshly prepared native OVA, it was noticed that not all the CTL response could be accounted for by the OVA$_{257-264}$ determinant (data not shown). A similar observation was made when OVA-specific CTL lines were primed in vitro by repeated stimulation of naive T cells using spleen cells loaded by electroporation with native OVA (Fig. 1 A). As shown in Fig. 1 A, T cells stimulated in this way were more effective at killing the OVA-transfectant EG7 than in killing EL-4 cells sensitized with OVA$_{257-264}$ peptide. This observation suggested the existence of CTLs recognizing additional OVA epitope(s) which were induced by delivering higher concentrations of OVA than used in other immunization protocols.
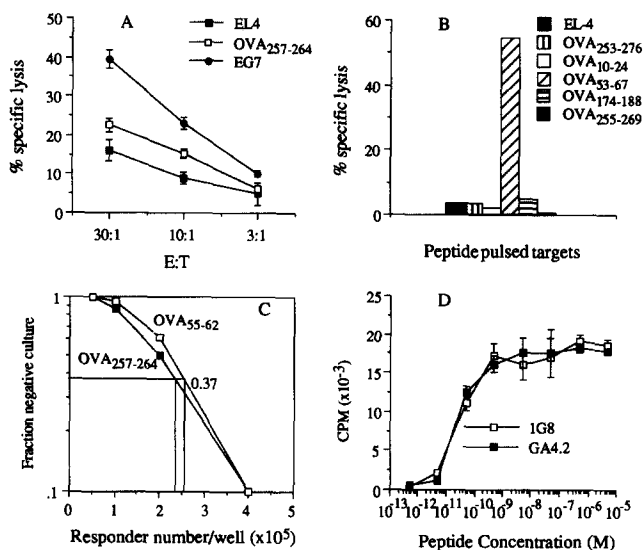

Figure 1. Identification of a new OVA determinant and comparison of CTLp frequencies. (A) 5 × 10^7 C57BL/6 spleen cells were cocultured with 5 × 10^7 irradiated syngeneic spleen cells loaded with 2 mg/ml OVA by electroporation in an upright T-25 flask. 5 d later the live cells were restimulated with the same APCs in the presence of 5 U/ml rIL-2 in 24-well plates. 5 d after the second restimulation, a 3.5-h ^{51}Cr-release assay was performed on EL-4 (■), EL-4 plus 0.5 μM OVA$_{257-264}$ (□), and OVA transfected EL-4 cell line EG7 (●). (B) A long-term CTL line from (A) was tested for cytotoxicity on EL-4 (■) or EL-4 plus 0.5 μM of the peptide OVA$_{253-276}$ (□), OVA$_{10-24}$ (□), OVA$_{53-67}$ (☒), OVA$_{174-188}$ (☒), or OVA$_{255-269}$ (▨). (C) For primed CTLp estimation, irradiated spleen cells (5 × 10^7) loaded with 5 mg/ml OVA by electroporation were reinjected intravenously into syngeneic mice. 10 d later the primed spleen cells were restimulated in microtiter plates at varying cell densities with 2.5 × 10^5 electroporated (5 mg/ml OVA) APCs as stimulators and the same number of irradiated spleen cells as feeders. 4 d later, 5 U/ml rIL-2 was added into the culture and the medium was renewed. Replicates were assayed by directly adding 10^4 ^{51}Cr-labeled RMA-S with 0.5 μM of OVA$_{257-264}$, 0.5 μM OVA$_{55-62}$, or without peptides in round-bottom plates. The CTLp frequencies were then determined as described in Materials and Methods. (D) To demonstrate the specificity and sensitivity of the T hybridomas GA4.2 and 1G8, I-3 cells (2 × 10^4) were pulsed with graded concentrations of peptides in 50 μl of FCS-free medium for 60 min at 37°C. The peptide-containing medium was then removed and the cells were washed three times with medium before either GA4.2 (OVA$_{257-264}$) or 1G8 (OVA$_{55-62}$) hybridoma cells (10^5) were added. IL-2 released in the supernatants was measured by CTLL after 24 h. Each point represents the mean value of triplicate assays.

In addition to the well-recognized OVA$_{257-264}$ determinant, at least five other peptide sequences containing the K^b-binding motif (x x x x F/Y x x L) proposed by Falk et al. (1) occur within the OVA Ag. These include OVA$_{12-19}$ (CFDVFKEL), OVA$_{25-32}$ (ENIFYCPI), OVA$_{55-62}$ (KVVRFDKL), OVA$_{107-114}$ (AEERYPIL), and OVA$_{176-183}$ (NAIVFKGL). A number of these peptides were therefore synthesized as 15-mer and tested for CTL recognition by addition to ^{51}Cr-labeled APCs. Although we expected that the optimal K^b-restricted peptides would be eight or nine residues in length, we felt that extracellular proteolysis would allow the evaluation of longer precursor peptides in initial screening for CTL activity. The reactivity of one CTL line was specific for a determinant contained in the synthetic peptide OVA$_{53-67}$ (Fig. 1 B), however CTLs recognizing other OVA determinants also may have been present within some uncloned CTL lines (data not shown). A simple explanation for the immunodominance of OVA$_{257-264}$ would be a higher frequency of CTLs capable of recognizing this determinant compared with other OVA peptides. To assess this possibility, the primed precursor frequencies of CTLs recognizing OVA$_{55-62}$ and OVA$_{257-264}$ were examined after immunization of H-2^b mice with OVA-electroporated syngeneic spleen cells. As shown in Fig. 1 C, the primed CTLp frequency in spleen cells from mice immunized with native OVA in vivo and restimulated under limiting dilution conditions in vitro, was similar for the OVA$_{257-264}$ and OVA$_{55-62}$ determinants (average result, 10^{-5}/spleen cell or ∼2.5 × 10^{-4}/T cell). Therefore the differences in the relative immunogenicity of OVA$_{257-264}$ and OVA$_{55-62}$ were not due to an obvious difference in the precursor repertoire of T cells reactive with these two determinants.

To evaluate presentation of the two OVA determinants in more detail, CTLs were fused to the CD8$^+$, "TCR-α^-/β^-" fusion-partner BW5147 and cloned T hybridomas which recognized K^b/OVA$_{55-62}$ were compared with the T hybridoma GA4.2, known to be specific for K^b/OVA$_{257-264}$ (46). One such T hybridoma, 1G8, was compared with GA4.2, as shown in Fig. 1 D. The 50% maximum IL-2 response of GA4.2 occurred at ∼50 pmol of synthetic OVA$_{257-264}$ similar to the concentration of synthetic OVA$_{55-62}$ required for 50% maximum response of the hybridoma 1G8 (Fig. 1 D).

Although most H-2K^b–restricted peptide fragments are octamers (1), some preferred peptides are nonamers (47). The OVA$_{257-264}$ peptide is known to be the optimal length of this determinant for K^b association (23, 46) as well as the peptide that is naturally presented by K^b molecules after OVA processing (48). The OVA$_{55-62}$ peptide was the preferred length for antigenicity of this determinant since lengthening of K^b-restricted peptides at the COOH terminus, and using peptides with longer or shorter NH$_2$ termini, resulted in one or more orders of magnitude impairment in stimulation by the T hybridoma 1G8 (data not shown) and in binding K^b molecules on RMA-S (data not shown, and see Fig. 4 B). We conclude that OVA$_{55-62}$ is the most likely naturally presented peptide derived from the OVA$_{53-67}$ determinant.

Presentation of OVA$_{257-264}$ Is More Efficient than OVA$_{55-62}$.

Because the dose–response curves of the hybridomas 1G8 (K^b/OVA$_{55-62}$) and GA4.2 (K^b/OVA$_{257-264}$) were quantitatively similar in experiments using synthetic peptides, relative differences in their activation on Ag-pulsed cells could conveniently be used to compare the relative presentation of OVA$_{257-264}$ and OVA$_{55-62}$ after natural Ag processing. These T hybridomas were therefore used to examine the natural appearance of the OVA$_{257-264}$ and OVA$_{55-62}$ determinants after the loading of native OVA into the cytoplasm of K^b-expressing APCs. It was previously shown (32) that OVA can be introduced into the cytoplasm of APCs by electroporation of cells in the presence of native OVA. Thus, splenic (Fig. 2 A) and L cell (Fig. 2 B) APCs were electroporated with graded amounts of freshly prepared native OVA, washed, and then cultured with GA4.2 or 1G8 for 24 h. Ag presentation was assessed by IL-2 production of the activated T hybridomas. To achieve 50% maximum activation of 1G8 it was necessary to load APCs with up to 50-fold higher concentrations of native OVA than required to give 50% maximum activation of GA4.2 (15 compared with 0.3 mg/ml, Fig. 2, A and B). Thus, the OVA$_{257-264}$ determinant was processed and/or presented up to 50 times more efficiently than the OVA$_{55-62}$ determinant after the cytoplasmic loading of native OVA. Ag presentation required cytoplasmic loading and processing of intact OVA and was not due to contaminating peptide fragments because APCs either pulsed with 20 mg/ml of OVA and then washed (Fig. 2 B), or electroporated in the presence of the same amount of OVA and washed before fixation with 1% paraformaldehyde (49) (Fig. 2 A), did not stimulate either T hybridoma. The difference in efficiency of presentation between OVA$_{257-264}$ and OVA$_{55-62}$ was between 20- and 50-fold in several types of APCs (including EL-4 cells; data not shown) and was also evident when OVA was introduced into APCs by different methods (e.g.,

by liposomes and osmotic loading; data not shown). In addition, neither the EL-4 OVA-transfected cell line EG7, nor the OVA-transfected K^b-expressing L cell (OVA1-1) activated the T hybridoma 1G8, despite activation of hybridoma GA4.2 by both of these cell lines (Fig. 2 C). Presumably, the level of K^b/OVA$_{55-62}$ expression by these OVA-expressing APCs was below the threshold for recognition by the T hybridoma 1G8, as suggested by the dose–response curves in Fig. 2, A and B.

Differences in the level of presentation of the OVA$_{55-62}$ and OVA$_{257-264}$ determinants might reflect differential Ag processing, peptide half-life, selective peptide importation into the ER/pre-Golgi, or differences in the affinity of peptide association with H-2K^b. Therefore, differences in the association of the two peptides with H-2K^b were evaluated to see if they could account for the differential Ag presentation of these determinants.

OVA$_{55-62}$ Associates much Less Efficiently with H-2K^b than OVA$_{257-264}$. The ability of OVA$_{55-62}$ and OVA$_{257-264}$ to associate with H-2K^b was examined by several methods. First, the capacity of the two synthetic peptide determinants to reciprocally inhibit T cell recognition was tested in functional assays using the hybridomas 1G8 and GA4.2 as reporters of K^b-peptide association. APCs were pulsed for 60 min at 37°C (in the absence of FCS) with the mixture of reporter peptide ($\sim$30 pmol) and graded concentrations of the competitor peptide to estimate the concentration required for 50% inhibition of the reporter response (Fig. 3, A and B). In several independent experiments, the concentration of OVA$_{55-62}$ needed to inhibit the response of GA4.2 to APC pulsed with OVA$_{257-264}$ was $\sim$2 × 10^{-7} M. In contrast, in the same experiments the concentration of OVA$_{257-264}$ needed to inhibit the response of 1G8 to APC pulsed with OVA$_{55-62}$ was $\sim$3 × 10^{-9} M. Thus, OVA$_{257-264}$ was considerably more effi-
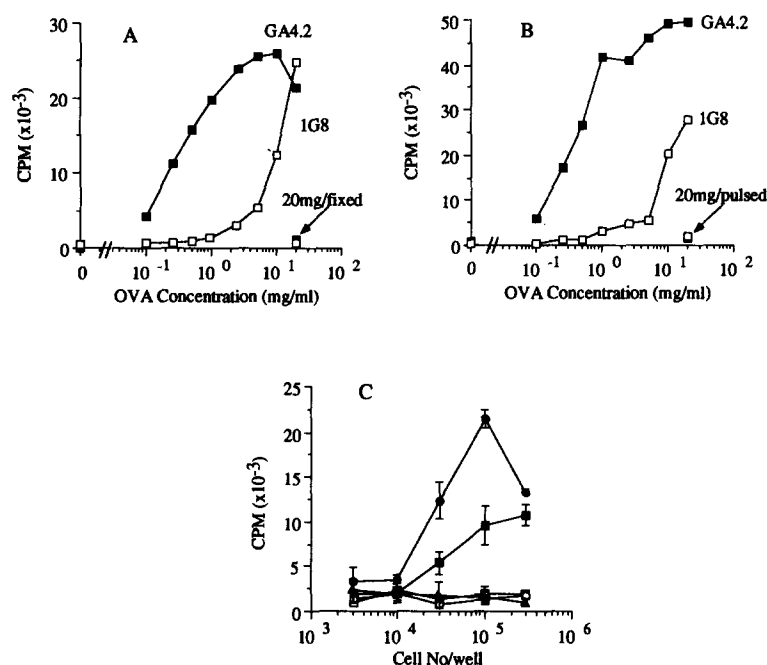
Figure 2. Presentation of OVA$_{257-264}$ derived from native OVA is more efficient than OVA$_{55-62}$. Irradiated spleen cells (A), and I-3 cells (B), were electroporated in the presence of graded concentrations of native OVA at 250 μF and 0.45 kV. The cells were then washed and assayed with 10^5 T hybridoma cells and 10^5 APC. Either 20 mg/ml OVA-pulsed APCs without electroporation (B), or APCs electroporated in the presence of 20 mg/ml OVA, then washed and fixed by 1% paraformaldehyde (A), were used to control for contaminating peptides or effects of electroporation on OVA antigen. Similar results were obtained with varying APC numbers. (C) 10^5 1G8 (*open symbols*) or GA4.2 (*closed symbols*) cells were cocultured with I-3 (*triangles*), OVA-transfected I-3 (*circles*), or OVA-transfected EL-4 (*squares*) at various APC densities. Each point represents the mean value of triplicate assays.
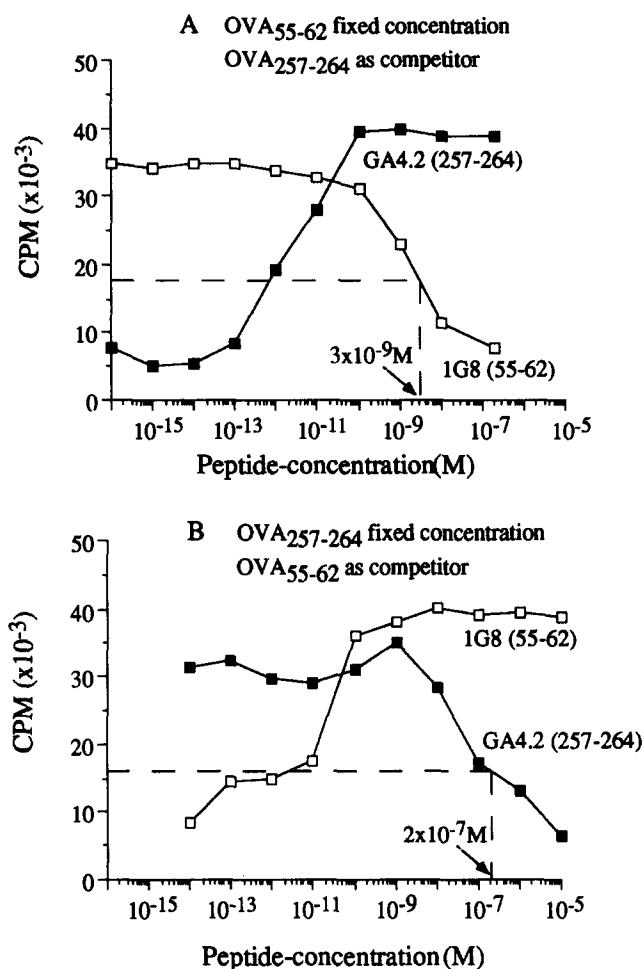
A

OVA$_{55-62}$ fixed concentration
OVA$_{257-264}$ as competitor

B

OVA$_{257-264}$ fixed concentration
OVA$_{55-62}$ as competitor

Figure 3. OVA$_{55-62}$ is less efficient at competing OVA$_{257-264}$ than vice versa. Either OVA$_{55-62}$ (A) or OVA$_{257-264}$ (B) was used to sensitize APCs at a final concentration of $\sim$3 × 10^{-11} M as stimulator peptide in DMEM free of FCS, with competitor peptide present at a range of concentrations as shown on the x-axis. The peptide mixture was directly added to I-3 cells in 96-well plates for 60 min at 37°C and the cells were washed three times before the addition of 10^5 of either hybridoma to each well. Peptide competition was assayed by activation of the T hybridomas 1G8 (□) and GA4.2 (■) after 24 h. The IL-2 content of the supernatants was measured by CTLL proliferation. Each point represents the mean value from duplicate assays and the complete experiment was repeated three times. The 50% inhibition concentration for each peptide is indicated with an arrow.

cient (60–70-fold) at competing recognition of K^b/OVA$_{55-62}$ than vice versa.

The ability of the two OVA peptides to stabilize surface expression of H-2K^b on the mutant APC RMA-S was then examined. The RMA-S cell line has defective TAP function and so fails to properly load class I molecules with peptide Ags derived from the cytoplasm. The association of peptide with thermolabile, empty-K^b molecules stabilizes these structures and results in an increase in the recognizable level of K^b on the cell surface of RMA-S which can then be stained by α1/α2 conformation-dependent mAbs such as Y-3 or 20.8.4 (17, 38, 39). This assay was used to quantitate the binding of the OVA$_{257-264}$ and OVA$_{55-62}$ peptides to K^b on

live RMA-S (Fig. 4). RMA-S cells were grown at 25°C overnight to induce high levels of empty K^b molecules which were then stabilized by pulsing with graded concentrations of the two OVA peptides. OVA-peptide binding to K^b was evident for both peptides with the 50% maximum values being $\sim$2.5 × 10^{-8} M for OVA$_{257-264}$, and $\sim$10^{-6} M for OVA$_{55-62}$ (Fig. 4 A). The differences in K^b-binding between the two synthetic peptides at 25°C was not the result of differential sensitivity to proteases in FCS since the functional activity of free peptide recovered at the completion of the assays (at 25°C) was similar for the two peptides (data not shown). The same relative K^b-peptide binding of OVA peptides was observed with independent K^b-specific mAb (including mAb Y-3 and 20.8.4) at 25°C, indicating that the differences in peptide–K^b association were not an artefact due to peptide-specific mAb (50–52). OVA$_{54-62}$ and OVA$_{56-62}$ peptides were even less efficient at associating with H-2K^b on RMA-S cells at 25°C, consistent with the conclusion that OVA$_{55-62}$ is the optimal length of the determinant for K^b-binding (Fig. 4 B). Taken together, the peptide competition and epitope induction/stabilization data suggested that the relative affinity of the K^b/OVA$_{257-264}$ complex was around 50-fold higher than that of the K^b/OVA$_{55-62}$ complex.

Differential K^b/OVA Peptide Binding Is Due to Kinetic Differences in both Association and Dissociation Rates. Variation in peptide–class I affinity has previously correlated with differences in dissociation rates of these complexes (21). Therefore, we estimated the relative rate of dissociation of K^b/OVA peptides by measuring the kinetic disappearance of antibody-reactive-K^b complexes on RMA-S formed overnight at 25°C, then washed of free peptide before being returned to 37°C. To minimize the effect of newly synthesized K^b molecules appearing on the cell surface during the decay period at 37°C, the RMA-S cells were cultured in the presence of BFA for the last 2.5 h of the peptide incubation and after the removal of peptides (41). BFA is an antifungal agent known to prevent the transport of newly synthesized class I molecules through the vacuolar compartment (53). As shown in Fig. 4 C, the $t_{1/2}$ for loss of empty-K^b expression at 37°C in the absence of any added peptide was <80 min whereas the $t_{1/2}$ for K^b molecules stabilized by OVA$_{257-264}$ was $\sim$470 min and for those stabilized by OVA$_{55-62}$, $\sim$160 min. Thus, at 37°C, peptide complexes of K^b/OVA$_{55-62}$ were lost from the cell surface of RMA-S at a rate two- to three times faster than complexes of K^b/OVA$_{257-264}$. This estimated difference in stability between K^b/OVA$_{55-62}$ and K^b/OVA$_{257-264}$ suggested that there must also be a significant difference in the association rate of the two peptides in order to fully account for the differences in presentation and epitope induction/stabilization of these two determinants. To test this hypothesis, we used a real time biosensor assay for measuring binding of OVA$_{55-62}$ and OVA$_{257-264}$ analogues to soluble secreted K^b molecules (H-2K^b$_s$) depleted of bound peptides by exposure to pH 12.5 (20). In this assay, OVA peptide analogues SIINFCKL (OVA$_{257-264}$-C6) and KVVRFCKL (OVA$_{55-62}$-C6) were coupled to a biosensor dextran–modified gold surface as previously described (20). The peptide residue at position 6 was chosen for Cys substitution because the side chain at
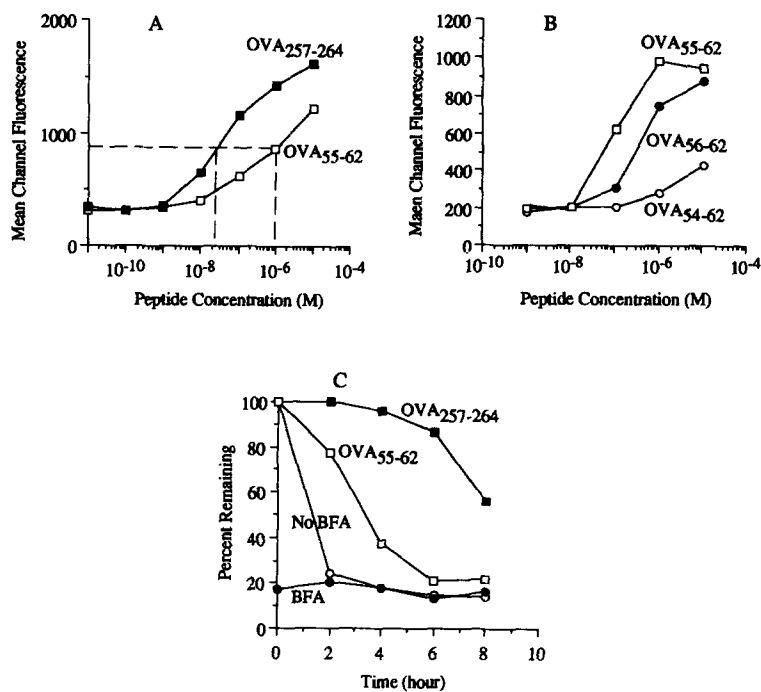
Figure 4. OVA$_{257-264}$ stabilizes K^b more efficiently than OVA$_{55-62}$. RMA-S cells (3 × 10⁵) were cultured in 24-well plates overnight (12–14 h) at 25°C and the indicated peptides were added for the last 60 min (*A* and *B*). The cells were then transferred to 37°C for 2 h and stained with an α1/α2 conformational mAb, Y3, and a FITC-labeled second Ab. (*C*) RMA-S cells (1.2 × 10⁶) were cultured at 25°C for 12 h in 12-well plates in the presence of 10 μM OVA$_{257-264}$ (■), OVA$_{55-62}$ (□), or in the absence of peptides, with (●) or without BFA (○). BFA (10 μg/ml) was added to all cultures for the last 2.5 h. The cells were then washed with prewarmed medium, aliquoted into 24-well plates in 0.3 ml DME-10 containing 10 μg/ml BFA, and transferred to 37°C. The transfer point was taken as time zero. Cell aliquots were sampled at different time points and stained as described above.

this position is known to be solvent exposed rather than directly engaged in K^b-binding. H-2K^b, injected into the flow chamber results in K^b-peptide binding at the dextran-modified gold surface which can be recorded instantaneously by a SPR detector. Plasmon resonance represents changes in the angle of complete internal reflectance of polarized light incident on the opposite surface of the gold film and is proportional to the mass of the material binding the modified surface.

The kinetic sensorgrams of binding of H-2K^b, to OVA$_{257-264-C6}$– and OVA$_{55-62-C6}$–modified biosensor surfaces are shown in Fig. 5. Binding experiments were carried out

at three concentrations of H-2K^b, and revealed significant kinetic differences in the association of H-2K^b, with OVA$_{257-264-C6}$ (Fig. 5, *A* and *C*) compared with OVA$_{55-62-C6}$ (Fig. 5, *B* and *C*). The OVA$_{257-264}$ analogue associated with an estimated K$_{on}$ of 5.9 × 10³ M^{-1} s^{-1} at 25°C whereas the OVA$_{55-62}$ analogue showed much slower binding to K^b, with an estimated K$_{on}$ of 6.5 × 10² M^{-1} s^{-1}. The association of K^b, with the OVA$_{257-264}$ analogue was biphasic whereas binding of the OVA$_{55-62}$ analogue was monophasic (compare Fig. 5, *A* and *B*). The reason for the apparent biphasic association of H-2K^b, with OVA$_{257-264-C6}$ is not clear, how-
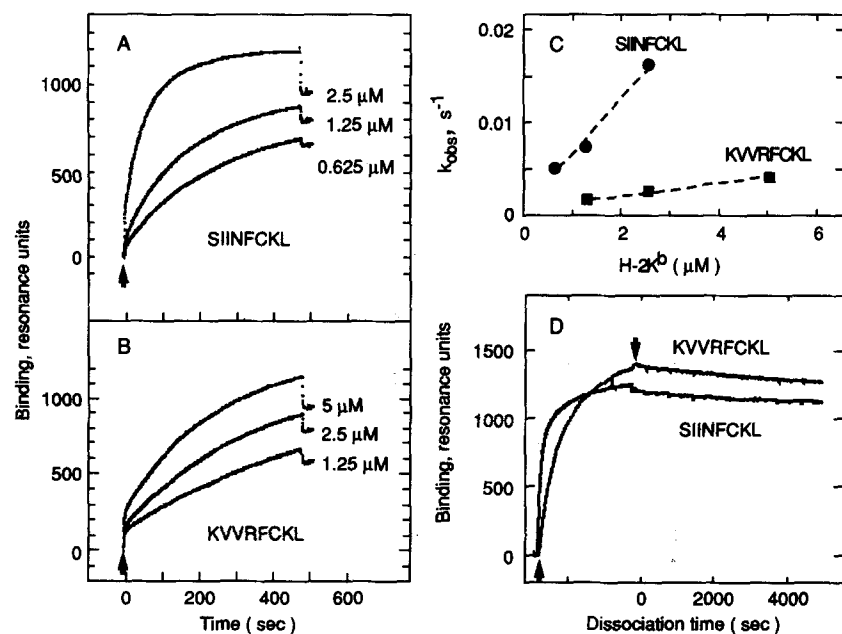

Figure 5. Measurement of K^b/peptide association and dissociation rate constants using SPR detection. H-2K^b, (0.625–5 μM) was injected over biosensor surfaces modified with SIINFCKL (OVA$_{257-264-C6}$) (*A*) or KVVRFCKL (OVA$_{55-62-C6}$) (*B*) for 8 min at a flow rate of 5 μl/min. (↓) Initiation of injection of the protein. (↓) Beginning of the buffer washout phase. Data points were curve fitted, as described in Materials and Methods. Values of K1$_{obs}$ were plotted versus H-2K^b, concentration (*C*), and curve fitted to a simple linear relationship, $y = mx + b$, in which $m = k_{as}$ in units of M^{-1} s^{-1}, and $b = k_{dis\ obs}$, in units of s^{-1}. Values for curve fitting are displayed. For measurement of dissociation rate constant using surface plasmon resonance detection (*D*), H-2K^b, (1.6 μM) was injected for 40 min at a flow rate of 1 μl/ml over biosensor surfaces modified with SIINFCKL (OVA$_{257-264-C6}$) or KVVRFCKL (OVA$_{55-62-C6}$) to apparent saturation, and the dissociation phase was followed during buffer washout at a flow rate of 100 μl/min. (↓ ↓) Beginning of protein and washout phases as described above. Data points were fitted to the double exponential decay equation as described in Materials and Methods. The dissociation kinetic rate constants obtained for the prevailing (slow) components are indicated in the text.

ever similar biphasic binding patterns have been observed for other MHC class I-peptide combinations (Khilko, S., and D. H. Margulies, unpublished results). Rapid MHC class I-peptide binding may occur with empty molecules, whereas slower binding could involve displacement of residual endogenously derived peptides from K^b molecules (54). Alternatively, biphasic binding might reflect peptide association with class I molecules at different stages of assembly with β_2-microglobulin.

The data demonstrate that H-2K^b_s was about 10-fold faster at associating with OVA$_{257-264}$-C6 compared with OVA$_{55-62}$-C6. This trend was preserved in binding experiments performed at 37°C though measurements at the higher temperature were complicated by a time-dependent denaturation of the protein (data not shown). These estimates of the association rate constants are of course dependent on the assumption that the H-2K^b_s protein preparations are completely active, that all binding sites are available for peptide binding, and that the C6-substituted analogues are representative of their parent peptides. The C6-substituted analogues stabilized K^b expression on RMA-S cells with equivalent efficiency to the wild-type peptides (data not shown), consistent with these analogues being closely representative of their parent peptides. Competitive inhibition in SPR binding assays also indicated that OVA$_{55-62}$-C6 was equivalent to OVA$_{55-62}$ in associating with H-2K^b_s, however H-2K^b_s was slightly less effective at binding OVA$_{257-264}$-C6 than wild-type OVA$_{257-264}$ (about twofold less). Thus, any discrepancy between the behavior of the C6-analogues and their parent sequences might serve to slightly underestimate the relative difference in K^b_s/OVA$_{257-264}$ and K^b_s/OVA$_{55-62}$ affinity constants in the solid phase SPR binding assay.

Kinetic dissociation of the K^b_s/OVA peptide analogues was measured at 25°C by washing out the K^b_s molecules after allowing K^b_s-peptide binding to reach saturation (Fig. 5 D). The results indicated that K^b_s/OVA$_{257-264}$-C6 dissociated with a $K_{off} = 9.1 \times 10^{-6}$ s^{-1} corresponding to a $t_{1/2} = 1,270$ min whereas for K^b_s/OVA$_{55-62}$-C6 the $K_{off} = 1.6 \times 10^{-5}$ s^{-1} corresponding to a $t_{1/2} = 720$ min. These relative dissociation rates (K^b_s/OVA$_{55-62}$-C6 K_{off} about twofold faster than K^b_s/OVA$_{257-264}$-C6) were consistent with the relative $t_{1/2}$ of surface K^b-peptide complexes determined in the RMA-S binding experiments shown in Fig. 4 C. An independent set of experiments using a different preparation of H-2K^b_s and with either OVA$_{257-264}$-C4 or OVA$_{55-62}$-C4 peptides immobilized on the biosensor surface, also indicated that OVA$_{55-62}$ associated more slowly and formed less stable complexes with H-2K^b_s than OVA$_{257-264}$ (data not shown). Thus, the biosensor studies demonstrate that the 20–50-fold difference in presentation and K^b-stabilization between OVA$_{257-264}$ compared with OVA$_{55-62}$ could be substantially accounted for by differences in both kinetic association (K^b_s/OVA$_{257-264}$-C6 $\geq$10-fold faster than K^b_s/OVA$_{55-62}$-C6) as well as kinetic dissociation (K^b_s/OVA$_{55-62}$-C6 $\geq$twofold faster than K^b_s/OVA$_{257-264}$-C6).

Multiple Peptide Residues As Well As Dominant Anchor Residues

Contribute to Class I–Peptide Association. Despite significant differences in K^b-binding of the OVA$_{55-62}$ and OVA$_{257-264}$ peptides, the sequences of these determinants contain very similar residues especially in the COOH-terminal half (OVA$_{257-264}$, SIINFEKL versus OVA$_{55-62}$, KVVRFDKL) where the K^b-binding motif residues 5F and 8L are located (1). In previous studies of K^b-peptide binding, P5 and P8 have been shown to be important for binding (33, 39), consistent with the observation that these residues are buried within the K^b-binding cleft (55, 56). Because the amino acids in these positions are identical between OVA$_{257-264}$ and OVA$_{55-62}$, we assumed the differences in their binding affinity for K^b must be due to other residues within the peptide sequences. Notably, the peptide residue at position 2 (or 3) has recently been suggested as another potential anchor site for K^b-binding (24). Therefore, to further evaluate the influence of individual residues in the interaction of the two OVA peptides with H-2K^b, reciprocally substituted peptide analogues of OVA$_{55-62}$ and OVA$_{257-264}$ were studied in RMA-S stabilization assays and competitively in T hybridoma activation assays. Table 1 shows the sequences of the wild-type peptides and their substituted analogues. The relative efficiency of K^b-peptide association is shown by normalizing the half-maximal peptide concentrations of each wild-type peptide to give a relative binding efficiency of 1. All peptide analogues containing single substitutions in the direction of OVA$_{55-62}$ → OVA$_{257-264}$ were capable of stabilizing K^b on RMA-S cells at 25°C. The substitutions of OVA$_{55-62}$ → OVA$_{257-264}$ at P1K → S, P2V → I, P4R → N, and P6D → E all resulted in K^b-stabilization which was significantly greater than that obtained with the parent peptide OVA$_{55-62}$ at 25°C. By contrast, substitution of OVA$_{55-62}$ → OVA$_{257-264}$ at P3V → I did not enhance K^b stabilization relative to the parent peptide OVA$_{55-62}$. The single most influential change in OVA$_{55-62}$ was the relatively conservative substitution P6D → E (OVA$_{55-62}$ → OVA$_{257-264}$) which resulted in 10-fold improvement in K^b-binding at 25°C relative to OVA$_{55-62}$. All of the peptide analogues in the set OVA$_{55-62}$ → OVA$_{257-264}$ showed some K^b-stabilizing ability at 37°C, which was not evident for wild-type OVA$_{55-62}$ under similar conditions.

Substituted analogues in the direction of OVA$_{257-264}$ → OVA$_{55-62}$ showed little or marginal impairment of K^b-binding evident at 37°C and all analogues from this set were still able to associate with K^b more efficiently than the OVA$_{55-62}$ peptide. The OVA$_{257-264}$ → OVA$_{55-62}$ substitution P6E → D was most disruptive for K^b binding requiring fivefold higher concentrations of peptide than the OVA$_{257-264}$ parent for 50% maximum binding at 25°C.

The OVA$_{55-62}$ → OVA$_{257-264}$ analogues which were most efficient at stabilizing K^b expression on RMA-S cells were also more effective than the OVA$_{55-62}$ parent peptide in competing T hybridoma recognition of OVA$_{257-264}$ reporter peptide (data not shown). Collectively, these findings indicate that amino acids other than the previously defined "anchor" residues, 5F and 8L, strongly influence the affinity of peptide–K^b association.

Discussion

One of the most intriguing questions arising from studies of class I–restricted immune responses is why so few peptide determinants are selected for recognition by CTLs despite the presence of other putative antigenic peptides within the same Ags (57–59). Even CTLs recognizing complex viral components including relatively large proteins such as envelope glycoproteins (60, 61), tend to focus the immune response on a small number of peptide determinants, leading to immunodominance of these peptides. Very little is known about the factors that influence immunodominance in the class I–restricted response, whereas the major influences on determinant selection and immunodominance in class II–restricted immune responses include the affinity of peptide–MHC association (11–13), differential Ag processing (62), and the presence of apparent holes in the T cell repertoire (13, 63). The stringent requirements for MHC class I–peptide binding (20, 25–27, 55, 56, 64–66) suggest that determinant selection in class I–restricted immune responses might be strongly influenced by the nature and strength of MHC class I–peptide binding. In this report we have compared the H-2K^b–restricted binding and presentation of the immunodominant OVA$_{257-264}$ (SIINFEKL) determinant to a subdominant OVA determinant, OVA$_{55-62}$ (KVVRFDKL). The novel feature of this study is the correlation between the hierarchical specificity of the in vivo class I–restricted response to OVA with the subsequent hierarchy of Ag presentation and the kinetic and biochemical details of K^b–peptide binding.

The mature immune response to OVA in H-2^b mice is dominated by CTLs recognizing K^b–OVA$_{257-264}$ complexes even though there are at least five peptide sequences within OVA that contain recognized K^b-binding motifs. In a study of mice immunized with OVA sequestered in immunostimulatory complexes (ISCOM) preparations, some uncloned CTLs recognized OVA$_{176-183}$ but it was unclear whether these CTLs recognized the OVA-transfected EG7 cells. This is the only study of which we are aware that identifies a K^b-restricted OVA determinant other than OVA$_{257-264}$ (59). It is notable that the OVA$_{176-183}$ determinant associates with K^b less efficiently than OVA$_{55-62}$ (33, 59, and data not shown). In our experience (Chen, W., and J. McCluskey) priming mice with the OVA-transfectant EG7, or by osmotic loading spleen cells with OVA, invariably leads to K^b-restricted CTLs recognizing only OVA$_{257-264}$. By contrast, when mice are primed by spleen cell electroporation using high concentrations (>2 mg/ml) of native OVA, K^b-restricted CTLs of mixed specificity can be elicited. Some of these CTLs recognize the OVA$_{55-62}$ determinant which we have studied in detail. The equivalent stoichiometry of OVA$_{257-264}$ and OVA$_{55-62}$ within native OVA allowed us to directly compare the presentation of the two determinants after Ag processing. Cytoplasmic loading of APCs with native OVA resulted in dose-dependent presentation of the OVA$_{257-264}$ at between 20- and 50-fold greater efficiency than the OVA$_{55-62}$ determinant. The dose-dependent increase in expression of the two OVA determinants indicates that the Ag processing and pep-

tide import mechanisms were not limiting for presentation of either OVA determinant (Fig. 2, A and B). Moreover, the rate of appearance of the two OVA determinants was identical in APCs that were electroporated in the presence of OVA, washed, and then fixed at different time points (data not shown), suggesting similar kinetics of TAP-dependent import into the ER. Nonetheless it is not possible to formally rule out the possibility that differences in the catabolic half-life of the two OVA determinants or subtle differences in TAP importation might also contribute to the relative Ag presentation of OVA$_{257-264}$ and OVA$_{55-62}$.

The OVA$_{55-62}$ determinant is likely to be the optimal length for presentation of this epitope and probably represents the naturally presented Ag because peptides that were shorter or longer than OVA$_{55-62}$ were poorly recognized by OVA-specific T hybridomas and bound very inefficiently to K^b molecules on RMA-S cells. However, formal proof that the OVA$_{55-62}$ peptide is naturally presented would require elution of this peptide from K^b molecules on APCs, followed by sequence or mass analysis of the peptide eluate. The OVA$_{257-264}$ peptide eluted from EG7 has been estimated to be present at <100 molecules/cell (48). Therefore, elution of the less efficiently presented OVA$_{55-62}$ peptide is unlikely to be feasible with current methodologies.

The OVA$_{257-264}$ peptide (50%$_{max}$-binding $\sim$25 nM) was $\sim$40-fold more efficient at stabilizing K^b on the surface of RMA-S cells than the OVA$_{55-62}$ peptide (50%$_{max}$-binding $\sim$1 μM) at 22–25°C. This difference in "affinity" for K^b was reflected in part in the greater instability of induced K^b/OVA$_{55-62}$ ($t_{1/2}$ = 2.7 h) complexes compared with K^b/OVA$_{257-264}$ ($t_{1/2}$ = 8.3 h) complexes at 37°C. These estimates of K^b–peptide stability probably reflect relative dissociation rates and are consistent with the K$_{off}$ values corresponding to $t_{1/2}$ = 3 h found in studies of nonamer peptides binding to K^d at 37°C (21) but are considerably longer than $t_{1/2}$ values of 2 min for radiolabeled OVA$_{257-264}$ analogue bound to K^b (59) and $t_{1/2}$ = 9.3 min for iodinated 17 mer bound to D^b (22). One of the inherent problems in estimating relative peptide–MHC class I affinities using the RMA-S K^b-stabilization assay is the inability to distinguish direct kinetic differences in off rate and on rate (24). For this reason, we studied the kinetic binding of OVA peptide analogues using biosensor techniques in which octameric OVA peptides were altered at position 6 where structural studies demonstrate the side chain to be solvent exposed and not directly involved in MHC class I–peptide binding. Relative dissociation rates of purified K^{b}s from OVA$_{257-264}$ and OVA$_{55-62}$ analogues calculated from plasmon resonance studies (K^{b}s/OVA$_{55-62-C6}$ dissociates about two times faster than ^{b}s/OVA$_{257-264-C6}$) were in agreement with estimates derived from RMA-S epitope induction/stabilization experiments. However, the most striking difference in the two OVA peptides was in their relative kinetic association rates with K^b. Here the two peptides differed by 10-fold or more at 25°C implying a critical role for rapid association of peptides with MHC class I molecules to achieve efficient Ag presentation.

The values of K_{on} for K^b_s/OVA$_{257-264-C6}$ at 25°C (5.9 × 10³ $M^{-1} s^{-1}$) and K^b_s/OVA$_{55-62-C6}$ (6.5 × 10² $M^{-1} s^{-1}$) are comparable to the values of 1,140 $M^{-1} s^{-1}$ obtained for binding of radiolabeled nonameric peptides to empty single chain K^d molecules at 37°C (25) and 720 $M^{-1} s^{-1}$ for radiolabeled 17 mer bound to D^b molecules on EL-4 cells (22).

The difference in affinity of K^b_s and the OVA$_{257-264}$ (K_d = 1.56 × 10⁻⁹ M) and OVA$_{55-62}$ (K_d = 2.46 × 10⁻⁸ M) analogues was 16-fold as measured by the biosensor assay, however the C6-substituted analogue of OVA$_{257-264}$ may slightly underestimate the affinity of K^b/OVA$_{257-264}$. Therefore, these differences in K^b-peptide affinity are probably sufficient to account for most or all of the 20–50-fold differences in presentation of the two OVA determinants. The physiological relevance of kinetic differences in MHC class I–peptide binding is likely to vary at different stages of the Ag presentation pathway. For example in the ER, where MHC class I–peptide assembly is thought to take place, the short half-life of many peptides would require rapid association with class I molecules for successful presentation at the cell surface. The advantage of a fast on rate would be exaggerated because of competition between different peptides and the possible requirement for displacement of calnexin from newly formed class I–calnexin complexes (67, 68). However, once MHC class I–peptide complexes are formed they must remain stable long enough for transport to the cell surface (~30–45 min [69]) and then persist for a time sufficient to allow T cell recognition. Although higher affinity peptides will be favored in Ag presentation, the kinetics of MHC class I–peptide binding need to meet this balance. The results obtained with the OVA$_{257-264}$ and OVA$_{55-62}$ peptides define a threshold of MHC class I–peptide affinity corresponding to an observed

bias in determinant selection and relative immunodominance of the OVA$_{257-264}$ determinant in the anti-OVA CTL response in vivo.

Despite the differences in K^b-binding affinity of OVA$_{257-264}$ and OVA$_{55-62}$ both peptides contain the recognized "binding motif" for peptide association with K^b (1) and possess conserved amino acids between the flanking 5F and 8L anchor residues (FEKL versus FDKL). K^b-binding of systematically substituted analogues of the two peptides indicated that multiple residues controlled the difference in K^b-binding between the two OVA peptides. For example, substitution of P2V → I in OVA$_{55-62}$ improved K^b-binding of this peptide fourfold, consistent with the side chain of isoleucine interacting more efficiently with the K^b-B/D pockets than the shorter side chain of valine (24, 55, 56). Accordingly, some perceived "nonanchor" residues may in fact be acting as minor anchor sites exerting considerable influence on Ag presentation (24). Some of the OVA$_{55-62}$ → OVA$_{257-264}$ changes involved residues where the side chains are predicted to be solvent exposed and not directly involved in binding to K^b. For example the substitutions of OVA$_{55-62}$ at P6D → E and P4R → N both enhanced stabilization of K^b even though side chains at these positions are thought to lie outside the K^b cleft where they are accessible to the TCR. These findings support the idea that conformational changes within the peptide Ag might exert considerable influence on MHC class I–peptide stability. The summation of enhanced K^b-binding of individual OVA$_{55-62}$ → OVA$_{257-264}$ analogues shown in Table 1 adds up to a 160-fold enhancement as OVA$_{55-62}$ is substituted towards OVA$_{257-264}$. However, the observed difference between K^b/OVA$_{55-62}$ and K^b/OVA$_{257-264}$ binding is considerably less than this. Therefore the data emphasize

Table 1. *Relative Ability of OVA Peptide Analogues to Stabilize H-2K^b*

Peptide		Amino Acid	Efficiency of peptide-binding to K^b	
			37°C (M)	25°C (M)
OVA$_{55-62}$		KVVRFDKL	− (>10⁻⁵)	1 (~10⁻⁶)*
OVA$_{55-62}$/P1K	→ S	S - - - - - - -	+	2
OVA$_{55-62}$/P2V	→ I	- I - - - - - -	+	4
OVA$_{55-62}$/P3V	→ I	- - I - - - - -	+	1
OVA$_{55-62}$/P4R	→ N	- - - N - - - -	+	2
OVA$_{55-62}$/P6D	→ E	- - - - - E - -	+	10
OVA$_{257-264}$		S I I NFEKL	1 (~2.5 × 10⁻⁶)	1 (~2.5 × 10⁻⁸)
OVA$_{257-264}$/P1S	→ K	K - - - - - - -	0.4	1
OVA$_{257-264}$/P2I	→ V	- V - - - - - -	1.2	1.2
OVA$_{257-264}$/P3I	→ V	- - V - - - - -	0.5	1
OVA$_{257-264}$/P4N	→ R	- - - R - - - -	0.4	1
OVA$_{257-264}$/P6E	→ D	- - - - - D - -	0.4	0.2

* The concentration of peptide required to give 50% maximum stabilization of K^b on RMA-S cells has been normalized to a binding efficiency of 1. Values >1 indicate more efficient K^b stabilization and values <1 indicate less efficient K^b binding. The actual 50% maximum peptide concentrations for binding were OVA$_{55-62}$ = 10⁻⁶ M, OVA$_{257-264}$ = 2.5 × 10⁻⁸ M at 25° C and OVA$_{55-62}$ >10⁻⁵ M, OVA$_{257-264}$ = 2.5 × 10⁻⁶ M at 37° C.

that the contribution of each residue to MHC class I–peptide binding is not simply additive and instead is dependent upon the sequence context.

Thus, the association of peptide Ags with class I molecules can be highly sequence dependent despite the presence of conserved allele-specific binding motifs (26, 28, 33, 47). This latter finding contrasts with binding studies of poly-alanine-substituted peptides showing MHC class I–peptide binding energy is controlled almost entirely by anchor residues and interaction with the peptide backbone (24). It is likely that the use of alanine substitutions to study the contributions of individual amino acids to peptide–MHC class I binding will minimize peptide side chain influences and potentially obscure detection of side chain interactions occurring between different peptide residues (70). In our studies, the contribution of "nonmotif" residues (e.g., P2 and P6) was shown to influence the affinity of peptide–MHC class I interaction where dominant anchor sites were conserved. Most importantly, these differences in MHC class I–peptide binding correspond with the outcome of the immune response and demonstrate that subtle influences at this level can influence physiological Ag presentation and the hierarchy of determinant selection in vivo.

Taken together, these data indicate that immunodominance of OVA$_{257-264}$ and subdominance of the OVA$_{55-62}$ epitopes within OVA are largely accounted for by kinetic differences in class I–peptide association resulting in affinity variation and differential Ag presentation. This difference in K^b–peptide association results from the contribution of multiple peptide side chains rather than altered "dominant anchor" residues and suggests considerable complexity in the rules governing class I–peptide association.

References

1. Falk, K., O. Rotzschke, S. Stevanovic, G. Jung, and H.-G. Rammensee. 1991. Allele-specific motifs revealed by sequencing of self-peptides eluted from MHC molecules. *Nature (Lond.).* 351:290.
2. Jardetzky, T.S., W.S. Lane, R.A. Robinson, D.R. Madden, and D.C. Wiley. 1991. Identification of self peptides bound to purified HLA-B27. *Nature (Lond.).* 353:326.
3. Guo, H.C., T.S. Jardetzky, T.P. Garrett, W.S. Lane, J.L. Strominger, and D.C. Wiley. 1992. Different length peptides bind to HLA-Aw68 similarly at their ends but bulge out in the middle. *Nature (Lond.).* 360:364.
4. Deverson, E.V., I.R. Gow, W.J. Coadwell, J.J. Monaco, G.W. Butcher, and J.C. Howard. 1990. MHC class II region encoding proteins related to the multidrug resistance family of transmembrane transporters. *Nature (Lond.).* 348:738.
5. Powis, S.J., A.R.M. Townsend, E.V. Deverson, J. Bastin, G.W. Butcher, and J.C. Howard. 1991. Restoration of antigen presentation to the mutant cell line RMA-S by an MHC-linked transporter. *Nature (Lond.).* 354:528.
6. Kelly, A., S.H. Powis, L.A. Kerr, I. Mockridge, T. Elliott, J. Bastin, B. Uchanska-Ziegler, A. Ziegler, J. Trowsdale, and A. Townsend. 1992. Assembly and function of the two ABC transporter proteins encoded in the human major histocompatibility complex. *Nature (Lond.).* 355:641.
7. Kleijmeer, M.J., A. Kelly, H.J. Geuze, J.W. Slot, A. Townsend, and J. Trowsdale. 1992. Location of MHC-encoded transporters in the endoplasmic reticulum and cis-Golgi. *Nature (Lond.).* 357:342.
8. Driscoll, J., M.G. Brown, D. Finley, and J.J. Monaco. 1993. MHC-linked LMP gene products specifically alter peptidase activities of the proteasome. *Nature (Lond.).* 365:262.
9. Shepherd, J.C., T.N. Schumacher, P.G. Ashton-Richardt, S. Imaeda, H.L. Ploegh, and C.A.J. Janeway. 1993. TAP1-dependent peptide translocation *in vitro* is ATP dependent and peptide selective. *Cell.* 74:577.
10. Neefjes, J.J., F. Momburg, and G.J. Hammerling. 1993. Selective and ATP-dependent translocation of peptides by the MHC-encoded transporter. *Science (Wash. DC).* 261:769.
11. Buus, S., A. Sette, S.M. Colon, G. Miles, and H.M. Grey. 1987. The relation between major histocompatibility complex (MHC) restriction and the capacity of Ia to bind immunogenic peptides. *Science (Wash. DC).* 235:1353.
12. Adorini, L., E. Appella, G. Doria, and Z.A. Nagy. 1988. Mechanisms influencing the immunodominance of T cell determinants. *J. Exp. Med.* 168:2091.
13. Schaeffer, E.B., A. Sette, D.L. Johnson, M.C. Bekoff, J.A. Smith, H.M. Grey, and S. Buus. 1989. Relative contribution of 'determinant selection' and 'holes in the T-cell repertoire' to T-cell responses. *Proc. Natl. Acad. Sci. USA.* 86:4649.
14. Chen, B., and P. Parham. 1989. Direct binding of influenza peptides to class I HLA molecules. *Nature (Lond.).* 337:743.
15. Choppin, J., F. Martinon, E. Gomard, E. Bahraoui, F. Connan, M. Bouillot, and J.-P. Levy. 1990. Analysis of physical interactions between peptides and HLA molecules and application

to the detection of human immunodeficiency virus 1 antigenic peptides. *J. Exp. Med.* 172:889.

16. Frelinger, J.A., F.M. Gotch, H. Zweerink, E. Wain, and A.J. McMichael. 1990. Evidence of widespread binding of HLA class I molecules to peptides. *J. Exp. Med.* 172:827.

17. Townsend, A., T. Elliott, V. Cerundolo, L. Foster, B. Barber, and A. Tse. 1990. Assembly of MHC class I molecules analyzed *in vitro*. *Cell.* 62:285.

18. Corr, M., L.F. Boyd, S.R. Frankel, S. Kozlowski, E.A. Padlan, and D.H. Margulies. 1992. Endogenous peptides of a soluble major histocompatibility complex class I molecule, H-2L^{d}s: sequence motif, quantitative binding, and molecular modelling of the complex. *J. Exp. Med.* 176:1681.

19. Wettstein, P.J., G.M. van Bleek, and S.G. Nathenson. 1993. Differential binding of a minor histocompatibility antigen peptide to H-2 class I molecules correlates with immune responsiveness. *J. Immunol.* 150:2753.

20. Khilko, S.N., M. Corr, L.F. Boyd, A. Lees, J.K. Inman, and D.H. Margulies. 1993. Direct detection of major histocompatibility complex class I binding to antigenic peptides using surface plasmon resonance. *J. Biol. Chem.* 268:15425.

21. Cerundolo, V., T. Elliott, J. Elvin, J. Bastin, H.-G. Rammensee, and A. Townsend. 1991. The binding affinity and dissociation rates of peptides for class I major histocompatibility complex molecules. *Eur. J. Immunol.* 21:2069.

22. Christinck, E.R., M.A. Luscher, B.H. Barber, and D.B. Williams. 1991. Peptide binding to class I MHC on living cells and quantitation of complexes required for CTL lysis. *Nature (Lond.).* 352:67.

23. Matsumura, M., Y. Sailto, M.R. Jackson, E.S. Song, and P.A. Peterson. 1992. In vitro peptide binding to soluble empty class I major histocompatibility complex molecules isolated from transfected *Drosophila melanogaster* cells. *J. Biol. Chem.* 267:23589.

24. Saito, Y., P.A. Peterson, and M. Matsumura. 1993. Quantitation of peptide anchor residue contributions to class I MHC molecule binding. *J. Biol. Chem.* 268:21309.

25. Ojcius, D.M., F. Godeau, J.-P. Abastado, J.-L. Casanova, and P. Kourilsky. 1993. Real-time measurement of antigenic peptide binding to empty and preloaded single-chain major histocompatibility complex class I molecules. *Eur. J. Immunol.* 23:1118.

26. Ruppert, J., J. Sidney, E. Celis, R.T. Kubo, H.M. Grey, and A. Sette. 1993. Prominent role of secondary anchor residues in peptide binding to HLA-A2.1 molecules. *Cell.* 74:929.

27. Margulies, D.H., M. Corr, L.F. Boyd, and S.N. Khilko. 1993. MHC class I/peptide interactions: binding specificity and kinetics. *J. Mol. Recognit.* 6:59.

28. Parker, K.C., M.A. Bednarek, and J.E. Coligan. 1994. Scheme for ranking potential HLA-A2 binding peptides based on independent binding of individual peptide side-chains. *J. Immunol.* 152:163.

29. Karre, K., H. Ljunggren, G. Piontek, and R. Kiessling. 1986. Selective rejection of H-2-deficient lymphoma variants suggests alternative immune defence strategy. *Nature (Lond.).* 319:675.

30. Moore, M.W., F.R. Carbone, and M.J. Bevan. 1988. Introduction of soluble protein into the class I pathway of antigen processing and presentation. *Cell.* 54:777.

31. Burgert, H.-G., J. White, H.-U. Weltzien, P. Marrack, and J.W. Kappler. 1989. Reactivity of Vβ17α$^+$ CD8$^+$ T cell hybridomas. Analysis using a new CD8$^+$ T cell fusion partner.

J. Exp. Med. 170:1887.

32. Chen, W., F.R. Carbone, and J. McCluskey. 1993. Electroporation and commercial liposomes efficiently deliver soluble protein into MHC class I presentation pathway: priming in vitro and in vivo for class I-restricted recognition of soluble antigen. *J. Immunol. Methods.* 160:49.

33. Jameson, S.C., and M.J. Bevan. 1992. Dissection of major histocompatibility complex (MHC) and T cell receptor contact residues in a K^b-restricted ovalbumin peptide and an assessment of the predictive power of MHC-binding motifs. *Eur. J. Immunol.* 22:2663.

34. Langhorne, J., and K.F. Lindahl. 1981. Limiting dilution analysis of precursors of cytotoxic T lymphocytes. In Immunological Methods. Academic Press, Inc., New York. II:221.

35. Coligan, J.E., A.M. Kruisbeek, D.H. Margulies, E.M. Shevach, and W. Strober. 1992. Current Protocols In Immunology. Wiley Interscience, New York. 3.4.1.

36. Gillis, S., M.M. Ferm, W. Ou, and K. Smith. 1978. T cell growth factor: parameters of production and a quantitative microassay for activity. *J. Immunol.* 120:2027.

37. Bray, A.M., N.J. Maeji, and H.M. Geysen. 1990. The simultaneous multiple production of solution phase peptides; assessment of the Geysen method of simultaneous peptide synthesis. *Tetrahedron Lett.* 31:5811.

38. Ljunggren, H.-G., N.J. Stam, C. Ohlen, J.J. Neefjes, P. Hoglund, M.T. Heemels, J. Bastin, T.N.M. Schumacher, A. Townsend, K. Karre, and H.L. Ploegh. 1990. Empty MHC class I molecules come out in the cold. *Nature (Lond.).* 346:476.

39. Chen, W., J. McCluskey, S. Rodda, and F.R. Carbone. 1993. Changes at peptide residues buried in the major histocompatibility complex (MHC) class I binding cleft influence T cell recognition: a possible role for indirect conformational alterations in the MHC class I or bound peptide in determining T cell recognition. *J. Exp. Med.* 177:869.

40. Ozato, K., and D.H. Sachs. 1981. Monoclonal antibodies to mouse MHC antigens. III. Hybridoma antibodies reacting to antigens of H-2^b haplotype reveal genetic control of isotype expression. *J. Immunol.* 126:371.

41. Otten, G.R., E. Bikoff, R.K. Ribaudo, S. Kozlowski, D.H. Margulies, and R.N. Germain. 1992. Peptide and β$_2$-microglobulin regulation of cell surface MHC class I conformation and expression. *J. Immunol.* 148:3723.

42. Schneck, J., W.L. Maloy, J.E. Coligan, and D.H. Margulies. 1989. Inhibition of an allospecific T cell hybridoma by soluble class I proteins and peptides: estimation of the affinity of a T cell receptor for MHC. *Cell.* 56:47.

43. Jonsson, U., L. Fagerstam, B. Ivarsson, B. Johnsson, R. Karlsson, K. Lundh, S. Lofas, B. Persson, H. Roos, I. Ronnberg, et al. 1991. Real-time biospecific interaction analysis using surface plasmon resonance and a sensor chip technology. *Biotechniques.* 11:620.

44. Carbone, F.R., and M.J. Bevan. 1990. Class I-restricted processing and presentation of exogenous cell-associated antigen in vivo. *J. Exp. Med.* 171:377.

45. Nikolic-Zugic, J., and F.R. Carbone. 1990. The effect of mutations in the MHC class I peptide binding groove on the cytotoxic T lymphocyte recognition of the K^b-restricted ovalbumin determinant. *Eur. J. Immunol.* 20:2431.

46. Carbone, F.R., S.J. Sterry, J. Butler, S. Rodda, and M.W. Moore. 1992. T cell receptor α-chain pairing determines the specificity of residue 262 within the K^b-restricted, ovalbumin$_{257-264}$ determinant. *Int. Immunol.* 4:861.

47. Deres, K., T.N.M. Schumacher, K.-H. Wiesmuller, S. Stevanovic, G. Greiner, G. Jung, and H.L. Ploegh. 1992. Preferred size of peptides that bind to H-2K^b is sequence dependent. *Eur. J. Immunol.* 22:1603.

48. Rotzschke, O., K. Falk, S. Stevanovic, G. Jung, P. Walden, and H.-G. Rammensee. 1991. Exact prediction of a natural T cell epitope. *Eur. J. Immunol.* 21:2891.

49. Rock, K.L., L.E. Rothstein, S.R. Gamble, C. Gramm, and B. Benacerraf. 1992. Chemical cross-linking of class I molecules on cells creates receptive peptide binding sites. *J. Immunol.* 148:1451.

50. Bluestone, J.A., S. Jameson, S. Miller, and R. Dick II. 1992. Peptide-induced conformational changes in class I heavy chains alter major histocompatibility complex recognition. *J. Exp. Med.* 176:1757.

51. Čatipović, B., J.D. Porto, M. Mage, T.E. Johansen, and J.P. Schneck. 1992. Major histocompatibility complex conformational epitopes are peptide specific. *J. Exp. Med.* 176:1611.

52. Hogquist, K.A., A.G. Grandea III, and M.J. Bevan. 1993. Peptide variants reveal how antibodies recognize MHC class I. *Eur. J. Immunol.* 23:3028.

53. Nuchtern, J.G., J.S. Bonifacino, W.E. Biddison, and R.D. Klausner. 1989. Brefeldin A implicates egress from endoplasmic reticulum in class I restricted antigen presentation. *Nature (Lond.).* 339:223.

54. Ojcius, D.M., J.-P. Abastado, A. Casrouge, E. Mottez, L. Cabanie, and P. Kourilsky. 1993. Dissociation of the peptide-MHC class I complex limits the binding rate of exogenous peptide. *J. Immunol.* 151:6020.

55. Fremont, D.H., M. Matsumura, E.A. Stura, P.A. Peterson, and I.A. Wilson. 1992. Crystal structures of two viral peptides in complex with murine MHC class I H-2K^b. *Science (Wash. DC).* 257:919.

56. Matsumura, M., D.H. Fremont, P.A. Peterson, and I.A. Wilson. 1992. Emerging principles for the recognition of peptide antigens by MHC class I molecules. *Science (Wash. DC).* 257:927.

57. Bennink, J.R., and J.W. Yewdell. 1988. Murine cytotoxic T lymphocyte recognition of individual influenza virus proteins: high frequency of nonresponder MHC class I alleles. *J. Exp. Med.* 168:1935.

58. Pamer, E.G., J.T. Harty, and M.J. Bevan. 1991. Precise prediction of a dominant class I MHC-restricted epitope of *Listeria monocytogenes. Nature (Lond.).* 353:852.

59. Lipford, G.B., M. Hoffman, H. Wagner, and K. Heeg. 1993. Primary in vivo responses to ovalbumin. *J. Immunol.* 150:1212.

60. Bennink, J.R., J.W. Yewdell, G.L. Smith, and B. Moss. 1986. Recognition of cloned influenza virus hemagglutinin gene products by cytotoxic T lymphocytes. *J. Virol.* 57:786.

61. Takahashi, H., J. Cohen, A. Hosmalin, K.B. Cease, R. Houghten, J. Cornette, C. DeLisi, B. Moss, R.N. Germain, and J.A. Berzofsky. 1988. An immunodominant epitope of the HIV gp160 envelope glycoprotein recognized by class I MHC molecule-restricted murine cytotoxic T lymphocytes. *Proc. Natl. Acad. Sci. USA.* 85:3105.

62. Mamula, M.J. 1993. The inability to process a self-peptide allows autoreactive T cells to escape tolerance. *J. Exp. Med.* 177:567.

63. Sette, A., J. Sidney, F.C.A. Gaeta, E. Appella, S.M. Colon, M.-F. del Guercio, J.-C. Guery, and L. Adorini. 1993. MHC class II molecules bind indiscriminately self and non-self peptide homologs: effect on the immunogenicity of non-self peptides. *Int. Immunol.* 5:631.

64. Maryanski, J.L., J.-P. Abastado, and P. Kourilsky. 1987. Specificity of peptide presentation by a set of hybrid mouse class I MHC molecules. *Nature (Lond.).* 330:660.

65. Saper, M.A., P.J. Bjorkman, and D.C. Wiley. 1991. Refined structure of the human histocompatibility antigen HLA-A2 at 2.6Å resolution. *J. Mol. Biol.* 219:277.

66. van Bleek, G.M., and S.G. Nathenson. 1991. The structure of the antigen-binding groove of major histocompatibility complex class I molecules determines specific selection of self peptides. *Proc. Natl. Acad. Sci. USA.* 88:11032.

67. Degen, E., M.F. Cohen-Doyle, and D.B. Williams. 1992. Efficient dissociation of the p88 chaperone from major histocompatibility complex class I molecules requires both β_2-microglobulin and peptide. *J. Exp. Med.* 175:1653.

68. Ahluwalia, N., J.J. Bergeron, I. Wada, and E. Degen. 1992. The p88 molecular chaperone is identical to the endoplasmic reticulum membrane protein, calnexin. *J. Biol. Chem.* 267:10914.

69. Harding, C.V. 1992. Electroporation of exogenous antigen into the cytosol for antigen processing and class I major histocompatibility complex (MHC) presentation: weak base amines and hypothermia (18°C) inhibit the class I MHC processing pathway. *Eur. J. Immunol.* 22:1865.

70. Boehncke, W.-H., T. Takeshita, C.D. Pendleton, R.A. Houghten, S. Sadegh-Nasseri, L. Racioppi, J.A. Berzofsky, and R.N. Germain. 1993. The importance of dominant negative effects of amino acid side chain substitution in peptide-MHC molecule interactions and T cell recognition. *J. Immunol.* 150:331.